

Optical characterization of glass and glass- crystalline materials in the B_2O_3 - Bi_2O_3 - La_2O_3 system doped with Eu^{3+} ions

R. S. Iordanova¹, M. K. Milanova¹, L. I. Aleksandrov^{1*}, A. Khanna², N. Georgiev³

¹*Institute of General and Inorganic Chemistry, Bulgarian Academy of Sciences, G. Bonchev, str. bld. 11, 1113 Sofia, Bulgaria,*

²*Department of Physics, Guru Nanak Dev University, Amritsar, Punjab, India*

³*Department of Organic Synthesis and Fuels, University of Chemical Technology and Metallurgy, 8 Kl. Ohridski, 1756 Sofia, Bulgaria*

Received October 10, 2016; Revised November 10, 2016

Glass and glass-crystalline materials with nominal composition $55B_2O_3 \cdot 35Bi_2O_3 \cdot 10La_2O_3$ doped with 1 mol% Eu_2O_3 were synthesized by melt quenching method. Different phases were developed, applying several melting temperatures. According to the XRD data, glass-crystalline materials containing $LaBO_3$ as crystalline phase were obtained at 1050 °C and 1100 °C, while X-ray amorphous samples were prepared at 1200 °C. Thermal parameters of the obtained glass samples were estimated by DTA analysis. It was found that the thermal stability of the glass drastically increased with the addition of Eu_2O_3 (1 mol%). UV-Vis diffuse reflectance spectrum showed that the quenched glass is transparent in the visible region. $LaBO_3:Eu^{3+}$ crystals enhanced red ${}^5D_0-{}^7F_2$ photoluminescence emission of the glass-crystalline samples as compared with the glass sample. This is due to the incorporation of the active Eu^{3+} ions with low symmetry into the crystal phase.

Keywords: Glass; IR spectra; Luminescence spectra

INTRODUCTION

In the last decades, borate materials have largely demonstrated their potential for the development of new optoelectronics devices. Their interesting properties do not only limit to the crystalline phases but also can be extended to the glass form with different compositions [1]. In particular, remarkable attention has been directed towards complex bismuth-borate based glass systems, containing rare - earth metal oxides (RE) [1-3]. Such glasses have many technological applications as lenses, lasing materials, magneto-optic materials, optical-switching materials and sensors [1-3]. They have to possess, a high thermal stability, excellent surface polishing properties, high refractive index, etc. [1, 4] to be promising materials for use in all-optical devices. It has been reported that the glass structure of bismuth borate glasses can be stabilized by doping with RE oxides. In particular, $Bi_2O_3 \cdot B_2O_3$ glasses doped with suitable amount of La_2O_3 could tighten the glass network structure and improve the microhardness of bismuth-borate glass [2, 5, 6]. In this study, glass and glass-crystalline materials with

nominal composition $55B_2O_3 \cdot 35Bi_2O_3 \cdot 10La_2O_3$ doped with 1 mol% Eu_2O_3 have been prepared by melt quenching method. The influence of Eu^{3+} ions on the structure and optical properties of the $55B_2O_3 \cdot 35Bi_2O_3 \cdot 10La_2O_3$ glass has been also investigated.

EXPERIMENTAL

Reagent grade Bi_2O_3 , H_3BO_3 , La_2O_3 and Eu_2O_3 were used as starting materials to prepare one sample with nominal composition $55B_2O_3 \cdot 35Bi_2O_3 \cdot 10La_2O_3$ and three samples with the same nominal composition doped with 1 mol% Eu_2O_3 . The homogenized batches were melted at the temperature range between 1050-1200 °C for 30 min in a platinum crucible in air. The melts were quenched by pouring and pressing between two copper plates (cooling rates 10^1-10^2 K/s). The phase formation of the samples was established by x-ray phase analysis. Powder XRD patterns were registered at room temperature with a Bruker D8 Advance diffractometer using $Cu-K\alpha$ radiation. The data were obtained in the $10 < 2\theta < 60^\circ$ range with a step 0.02 for two different scanning times - of 0.02 seconds for the $55B_2O_3 \cdot 35Bi_2O_3 \cdot 10La_2O_3$ sample and at longer scanning time of 0.1 seconds

*To whom all correspondence should be sent:
E-mail: lubomirivov@gmail.com

for the three Eu_2O_3 doped specimens. Thermal parameters of the glasses were determined using differential thermal analysis (DTA) (Setaram, LabsysEvo 1600). The heating rate was 10K/min in air atmosphere under air flow of 20 mL/min. The IR spectra of the glasses were recorded in the 1600–400 cm^{-1} region, using the KBr pellet technique (Nicolet-320 FTIR spectrometer). The optical spectra of powder samples at room temperature were recorded with a spectrometer (Evolution 300 UV-vis Spectrophotometer) employing the integration sphere diffuse reflectance attachment. The uncertainty in the observed wavelength is about ± 1 nm. The Kubelka–Munk function ($F(R_\infty)$) was calculated from the UV–Vis diffuse reflectance spectra. The band gap energy (E_g) was determined by plot $(F(R_\infty) hv)^{1/n}$, $n = 2$ versus hv (incident photon energy). The photoluminescence (PL) spectra in the visible region of Eu^{3+} ions for the glass and glass–crystalline samples were recorded with PL spectrometer (Scinco FS-2 with wavelength accuracy 1 nm) at room temperature in which the excitation light of a wavelength $\lambda = 464$ nm was used.

RESULTS

Different phases were developed, applying several melting temperatures. According to the XRD data (Fig. 1 a, b, c, d), glass-crystalline materials containing LaBO_3 (JCPDS-00-012-0762) as crystalline phase were obtained at 1050 °C and 1100 °C, while x-ray amorphous samples were prepared at 1200°C. Visual observation of the obtained samples supported these experimental results. The two glasses $55\text{B}_2\text{O}_3 \cdot 35\text{Bi}_2\text{O}_3 \cdot 10\text{La}_2\text{O}_3$ and $55\text{B}_2\text{O}_3 \cdot 35\text{Bi}_2\text{O}_3 \cdot 10\text{La}_2\text{O}_3 : \text{Eu}^{3+}$ were dark brown and completely transparent. Glass-crystalline $55\text{B}_2\text{O}_3 \cdot 35\text{Bi}_2\text{O}_3 \cdot 10\text{La}_2\text{O}_3 : \text{Eu}^{3+}$ specimen obtained at 1100 °C was yellow and opaque, while the sample melted at 1050 °C was opaquer probably as a result of its higher crystallinity.

We used the IR spectroscopy in order to check the effect of addition of Eu_2O_3 in $55\text{B}_2\text{O}_3 \cdot 35\text{Bi}_2\text{O}_3 \cdot 10\text{La}_2\text{O}_3$ glass matrix (Fig. 2). As it is seen from the figure, there is no noticeable difference in the spectra of both glasses. They contain absorption peaks characteristic of the BO_3 (1360 cm^{-1} , 1290 cm^{-1} , 1190 cm^{-1} and 695 cm^{-1}); BO_4 (1020 cm^{-1} and 910 cm^{-1}) and BiO_6 (540 cm^{-1} and 480 cm^{-1}) structural groups [6-8]. In order to get more precise information about the europium ions effect on the glass structure, we deconvoluted glass spectra to check the relative population of

boron in different structural units (BO_3 and BO_4). Fig 3 (a, b) shows the deconvolution in Gaussian bands, of the investigated spectra. Each component

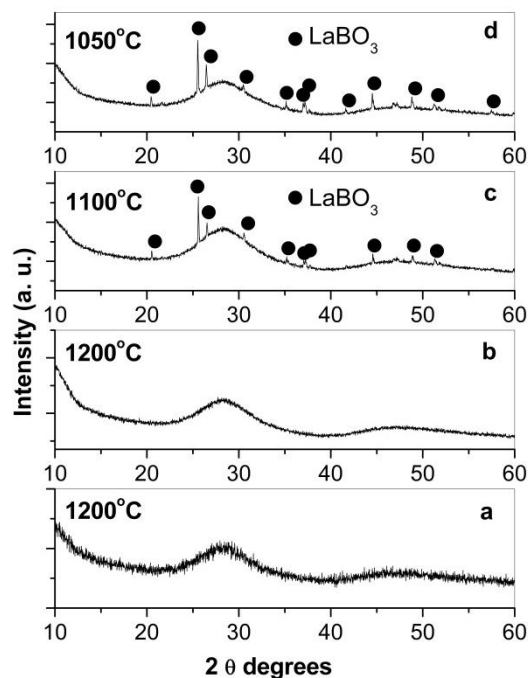


Fig. 1. XRD patterns of $55\text{B}_2\text{O}_3 \cdot 35\text{Bi}_2\text{O}_3 \cdot 10\text{La}_2\text{O}_3$ (a) and $55\text{B}_2\text{O}_3 \cdot 35\text{Bi}_2\text{O}_3 \cdot 10\text{La}_2\text{O}_3 : \text{Eu}^{3+}$ (b-d) glass and glass-crystalline samples obtained by melt quenching at different temperatures.

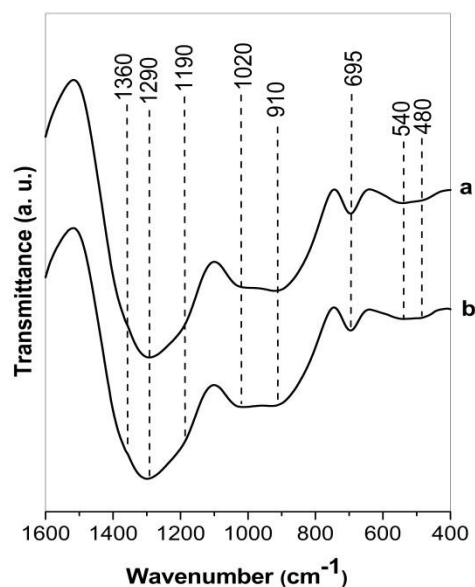


Fig. 2. IR spectra of $55\text{B}_2\text{O}_3 \cdot 35\text{Bi}_2\text{O}_3 \cdot 10\text{La}_2\text{O}_3$ (a) and $55\text{B}_2\text{O}_3 \cdot 35\text{Bi}_2\text{O}_3 \cdot 10\text{La}_2\text{O}_3 : \text{Eu}^{3+}$ (b) glass samples obtained by melt quenching technique.

band is related to some type of vibration in specific structural groups. The concentration of the structural group was considered to be proportional

to the relative area of its component band. The deconvolution parameters (the band centre at C and the relative area A) and the band assignments are given in Table 1. These characteristic parameters are used to calculate the fraction N_4 of BO_4 units in the bismuth-borate matrix. N_4 can be defined as the

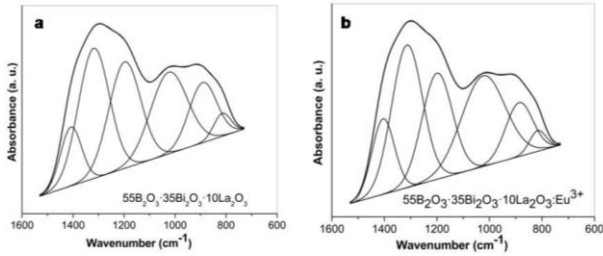


Fig. 3. Deconvoluted IR spectra of: (a) $55\text{B}_2\text{O}_3 \cdot 35\text{Bi}_2\text{O}_3 \cdot 10\text{La}_2\text{O}_3$ and (b) $55\text{B}_2\text{O}_3 \cdot 35\text{Bi}_2\text{O}_3 \cdot 10\text{La}_2\text{O}_3 : \text{Eu}^{3+}$ glass samples obtained by melt quenching technique.

Table 1. Deconvolution parameters (the band centers C and the relative area A) and the band assignments for the undoped and Eu^{3+} doped $55\text{B}_2\text{O}_3 \cdot 35\text{Bi}_2\text{O}_3 \cdot 10\text{La}_2\text{O}_3$ glass

Sample	C	A	Assignments	Ref.
$55\text{B}_2\text{O}_3 \cdot 35\text{Bi}_2\text{O}_3 \cdot 10\text{La}_2\text{O}_3$	815	2.8	B-O stretch vibration in BO_4 groups	6-8
	892	12.1	B-O stretch vibration in BO_4 groups	6-8
	1025	21.9	B-O stretch vibration in BO_4 groups	6-8
	1197	24.7	B-O stretch vibration in BO_3 groups	6-8
	1319	29.5	B-O stretch vibration in BO_3 groups	6-8
	1408	9.0	B-O stretch vibration in BO_3 groups	6-8
$55\text{B}_2\text{O}_3 \cdot 35\text{Bi}_2\text{O}_3 \cdot 10\text{La}_2\text{O}_3 \cdot \text{Eu}^{3+}$	816	2.2	B-O stretch vibration in BO_4 groups	6-8
	887	9.7	B-O stretch vibration in BO_4 groups	6-8
	1024	26.18	B-O stretch vibration in BO_4 groups	6-8
	1199	21.4	B-O stretch vibration in BO_3 groups	6-8
	1314	29.2	B-O stretch vibration in BO_3 groups	6-8
	1405	11.2	B-O stretch vibration in BO_3 groups	6-8

samples ratio of the concentration of BO_4 units to the concentration of $(\text{BO}_3 + \text{BO}_4)$ units [4, 8]. The calculated N_4 values for the studied compositions are 0.36 and 0.38 for the undoped and Eu^{3+} doped $55\text{B}_2\text{O}_3 \cdot 35\text{Bi}_2\text{O}_3 \cdot 10\text{La}_2\text{O}_3$ glass respectively. The higher N_4 values for the Eu^{3+} doped sample calculated reveals that the presence of europium ions influences the surroundings of the B^{3+} cations favouring the formation of the BO_4 structural units and in this way the glass network became more stable [8].

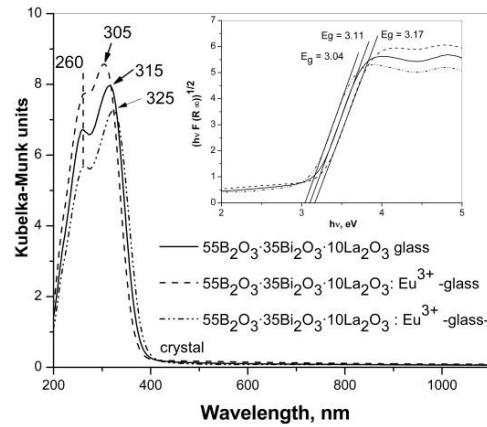


Fig. 4. DR-UV-Vis spectra and the band gap energy E_g (inset) of $55\text{B}_2\text{O}_3 \cdot 35\text{Bi}_2\text{O}_3 \cdot 10\text{La}_2\text{O}_3$ and $55\text{B}_2\text{O}_3 \cdot 35\text{Bi}_2\text{O}_3 \cdot 10\text{La}_2\text{O}_3 : \text{Eu}^{3+}$ glasses and $55\text{B}_2\text{O}_3 \cdot 35\text{Bi}_2\text{O}_3 \cdot 10\text{La}_2\text{O}_3 : \text{Eu}^{3+}$ glass-crystal obtained by melt quenching technique.

The structural modification of the $55\text{B}_2\text{O}_3 \cdot 35\text{Bi}_2\text{O}_3 \cdot 10\text{La}_2\text{O}_3$ glass network, caused by the presence of Eu_2O_3 is also evidenced by DR-UV-vis spectroscopy. Fig. 4 displays the diffuse reflectance spectra of undoped and Eu^{3+} doped $55\text{B}_2\text{O}_3 \cdot 35\text{Bi}_2\text{O}_3 \cdot 10\text{La}_2\text{O}_3$ glasses and $55\text{B}_2\text{O}_3 \cdot 35\text{Bi}_2\text{O}_3 \cdot 10\text{La}_2\text{O}_3 : \text{Eu}^{3+}$ glass-crystal. In all spectra, two absorption bands at 260 nm and 305-325 nm are observed. In the Eu^{3+} free spectrum these bands are due to $^1\text{S}_0 \rightarrow ^3\text{P}_1$ and $^1\text{P}_1$ transitions of Bi^{3+} ions [9, 10]. The higher absorption intensity in the spectrum of Eu^{3+} doped glass is a result of the contribution of ligand-to-metal charge-transfer band of Eu^{3+} ions (310-315 nm) [11, 12]. In addition, the band located at 315 nm in the spectrum of Eu^{3+} free glass slightly blue shifts to 305 nm in the presence of Eu_2O_3 . The observed spectral differences can be explained in terms of the structural changes that are taking place with the incorporation of the Eu^{3+} ions in the glass network [9, 10]. The shift towards lower wavenumber can be explained with the formation of more symmetrical EuO_6 and BiO_6 units [13]. Optical band gap values (E_g) evaluated from the UV-Vis spectra can also give information about the structural arrangement of the glasses under

investigation. The calculated band gap (E_g) energy values for indirect transition (see the inset in the Fig. 4) are 3.11 eV and 3.17 eV for the undoped and Eu^{3+} -doped $55\text{B}_2\text{O}_3\cdot 35\text{Bi}_2\text{O}_3\cdot 10\text{La}_2\text{O}_3$ glass respectively. According to the literature in glasses the variation of E_g may be attributed to the network structural changes [14, 15]. It is well known that in metal oxides, creation of non-bonding orbitals with higher energy than bonding ones shifts valence band to higher energy which results to E_g decreasing. However, in our case, E_g value of Eu^{3+} -doped glass increases which evidence that Eu_2O_3 improves the connectivity inside the network by decreasing of the non-bridging oxygen species. In the case of glass-crystalline Eu^{3+} doped sample, the band above 300 nm shifts to higher wavenumber – 325 nm and E_g value is lower – 3.04 eV. These spectral features indicate that Eu^{3+} ions are with lower local symmetry.

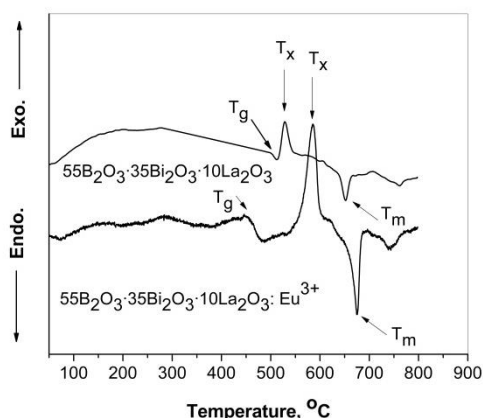


Fig. 5. DTA curves of $55\text{B}_2\text{O}_3\cdot 35\text{Bi}_2\text{O}_3\cdot 10\text{La}_2\text{O}_3$ and $55\text{B}_2\text{O}_3\cdot 35\text{Bi}_2\text{O}_3\cdot 10\text{La}_2\text{O}_3 : \text{Eu}^{3+}$ glass samples obtained by melt quenching technique.

The formation of more rigid glass structure with the addition of Eu_2O_3 is also confirmed by the DTA data obtained (Fig. 5). For the undoped $55\text{B}_2\text{O}_3\cdot 35\text{Bi}_2\text{O}_3\cdot 10\text{La}_2\text{O}_3$ glass, DTA shows a hump, corresponding to the glass transition temperature T_g at 505 °C, followed by one exothermic peak at 530 °C, corresponding to crystallization temperature - T_x and other endothermic event, corresponding to the melting temperature T_m – 650 °C. For the Eu^{3+} doped glass the glass transition temperature T_g is at 457 °C, exothermic peak of crystallization T_x at 590 °C and endothermic peak, corresponding to the melting temperature T_m at 680 °C. The temperature difference $\Delta T = T_x - T_g$, gives a measure of the thermal stability of a glass against crystallization is 25 °C and 133 °C for the undoped and Eu^{3+} doped glass respectively. As it is seen from the DTA data

obtained, Eu^{3+} doped glass has higher glass crystallization temperature T_x and possesses much higher thermal stability (higher ΔT) as compared with the undoped glass. These results suggest that the network structure of $55\text{B}_2\text{O}_3\cdot 35\text{Bi}_2\text{O}_3\cdot 10\text{La}_2\text{O}_3 : \text{Eu}^{3+}$ glass is becoming stronger with the introduction of Eu_2O_3 .

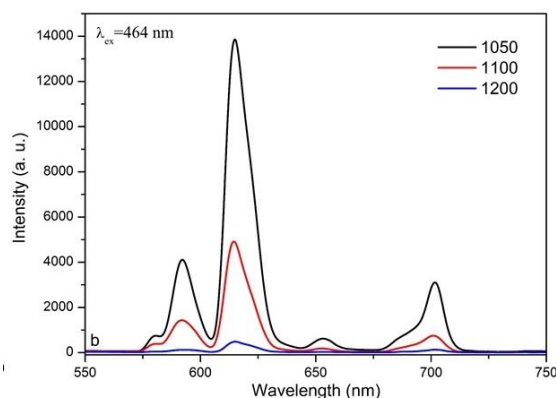
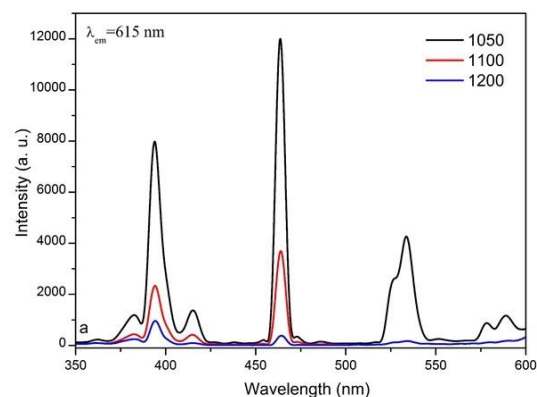


Fig. 6. PL (a) excitation and (b) emission spectra of $55\text{B}_2\text{O}_3\cdot 35\text{Bi}_2\text{O}_3\cdot 10\text{La}_2\text{O}_3 : \text{Eu}^{3+}$ glass and glass-crystal samples obtained by melt quenching technique at different temperatures.

The PL excitation and emission spectra at room temperature for prepared $55\text{B}_2\text{O}_3\cdot 35\text{Bi}_2\text{O}_3\cdot 10\text{La}_2\text{O}_3 : \text{Eu}^{3+}$ glass and glass-crystals are shown on Fig. 6 a and b. The monitoring of excitation spectra (Fig. 6a) shown that the intensity of the absorption peak at 464 nm dominates in comparison with the intensity of the absorption at 394 nm. That is why the emission was registered with excitation at 464 nm. The emission spectra (Fig. 6b) excited at $\lambda_{\text{ex}}=464$ nm consist five peaks assigned to the 4f transitions of Eu^{3+} ions, i.e., ${}^5\text{D}_0 \rightarrow {}^7\text{F}_J$ ($J=0, 1, 2, 3$ and 4). It is seen that the peaks intensity for sample melted at 1050°C dominate as compared to the other samples because of its higher degree of crystallinity. It is well known that the ${}^5\text{D}_0 \rightarrow {}^7\text{F}_1$ transition situated around orange light (590 nm) is due to the magnetic dipole transition while

$^5D_0 \rightarrow ^7F_2$ with red line (615 nm) corresponds to the electric dipole transition which band is dominant in all spectra [16, 17]. The ratio of integrated emission peaks intensity of the $^5D_0 \rightarrow ^7F_2$ transition to that of the $^5D_0 \rightarrow ^7F_1$ transition can be connected with the covalent/ionic bonding between Eu^{3+} ions and surrounding ligands. The increasing ratio value is due to the increasing of asymmetry between europium and oxygen ions [17]. For the sample synthesized at 1050 °C the calculated value is 0.25 while for the glass sample decrease to 0.15. These values indicate that Eu^{3+} ions are with lower local symmetry in the glass crystalline sample and they are in agreement with the DR-UV-vis results.

CONCLUSIONS

Glass and glass crystalline materials with nominal composition $55B_2O_3 \cdot 35Bi_2O_3 \cdot 10La_2O_3$ doped with 1 mol% Eu_2O_3 were synthesized by melt quenching technique and the influence of Eu^{3+} on the structure and optical properties of the glasses was investigated. The IR studies revealed the existence of BO_3 , BO_4 and BiO_6 as the main structural units of the amorphous network. Europium ions generate structural changes, favoring the formation of the BO_4 units. The optical absorption studies revealed that the optical band gap energy (E_g) of glasses increases in the presence of Eu^{3+} ions, while E_g of glass crystalline sample decreases. Increase in E_g value evidence the decrease in number of non-bridging oxygen ions in the glass structure. DTA data showed that the introduction of Eu_2O_3 significantly improves thermal stability of $55B_2O_3 \cdot 35Bi_2O_3 \cdot 10La_2O_3$ glass. $LaBO_3 \cdot Eu^{3+}$ crystals enhanced red $^5D_0 \rightarrow ^7F_2$ photoluminescence emission of the glass-crystalline samples as compared to the glass sample.

Acknowledgment: The study was performed with the financial support of The Ministry of Education and Science of Bulgaria, Contract No ДНТC/India 01/6, 2013: Bulgarian-Indian Inter-governmental Programme of Cooperation in Science and Technology.

REFERENCES

1. P. Yasaka, J. Kaewkhao, 2015 4th International Conference on Instrumentation, Communications, Information Technology, and Biomedical Engineering (ICICI-BME), Bandung, pp. 4, (2015), doi: 10.1109/ICICI-BME.2015.7401304.
2. M.A. Marzouk, *J. Molec. Struct.*, **1019**, 80 (2012).
3. A. Bajaj, A. Khanna, N. K. Kulkarni, S. K. Aggarwal, *J. Am. Ceram. Soc.*, **92**, 1036 (2009).
4. M. Farouk, A. Samir, F. Metawe, M. Elokr, *J. Non-Cryst. Solids*, **371-372**, 14 (2013).
5. Y. Cheng, H. Xiao, W. Guo, *Ceram. Int.*, **34**, 1335 (2008).
6. Y. Cheng, H. Xiao, W. Guo, *Mater. Sci. Eng. A*, **480**, 56 (2008).
7. E. I. Kamitsos, M. A. Karakassides, G. D. Chryssikos, *J. Phys. Chem.*, **91**, 1067 (1987).
8. P. Pascuta, S. Rada, G. Borodi, M. Bosca, L. Pop, E. Culea, *J. Mol. Struct.*, **924-926**, 214 (2009).
9. A. Sontakke, A. Tarafder, K. Biswas, K. Annapurna, *Phys. B*, **404**, 3525 (2009).
10. C. Kim, H. Park, S. Mho, *Solid State Commun.*, **101**, 109 (1997).
11. M. Gusik, E. Tomaszewicz, S. M. Kaczmarek, J. Cybińska, H. Fuks, *J. Non-Cryst. Sol.*, **356**, 1902 (2010).
12. C. A. Kodaira, H. F. Brito, O. L. Malta, O. A. Serra, *J. Lumin.*, **101**, 11 (2003).
13. E. I. Ross-Medgaarden, I. E. Wachs, *J. Phys. Chem. C*, **11**, 15089 (2007).
14. R. Jose, T. Suzuki, Y. Ohishi, *J. Non-Cryst. Solids*, **352**, 5564 (2006).
15. S. Rani, S. Sanghi, N. Ahlawat, A. Agarwal, *J. Alloys Comp.*, **597**, 110 (2014).
16. Y. Zhou, J. Xu, Z. Zhang, M. You, *J. Alloys Comp.*, **615**, 624 (2014).
17. J. Pisarska, L. Zur, W. A. Pisarsky, *Opt. Fibers Their Applic.*, **8010**, 80100N1 (2011).

ОПТИЧНО ОХАРАКТЕРИЗИРАНЕ НА ДОТИРАНИ С Eu^{3+} ЙОНИ, СТЪКЛА И СТЪКЛОКРИСТАЛНИ МАТЕРИАЛИ В СИСТЕМАТА $\text{B}_2\text{O}_3\text{-Vl}_2\text{O}_3\text{-La}_2\text{O}_3$

Р. С. Йорданова¹, М. К. Миланова¹, Л. И. Александров¹, А. Канна², Н. Георгиев³

¹*Институт по обща и неорганична химия, Българска академия на науките, ул. Г. Бончев, бл. 11, 1113
София, България, *e-mail: lubomirivov@gmail.com*

²*Университет Гуру Нанак Деф, Амритсар, Пенджаб, Индия*

³*Химикотехнологичен и металургичен университет, ул. Климент Охридски 8, 1756 София, България*

Постъпила на 10 октомври 2016 г.; коригирана на 10 ноември, 2016 г.

(Резюме)

По метода на преохладена стопилка, са синтезирани стъкла и стъклокристални материали с номинален състав $55\text{B}_2\text{O}_3\cdot 35\text{Vl}_2\text{O}_3\cdot 10\text{La}_2\text{O}_3$, дотирани с 1 мол.% Eu_2O_3 . В зависимост от приложената температура на топене, са получени различни фази. Според данните от рентгенофазовият анализ, са получени стъклокристални материали, съдържащи LaVO_3 като кристална фаза при 1050 °С и 1100 °С, докато при 1200°С е синтезиран рентгено-аморфен образец. Термичните параметри на получените стъкла, са определени чрез диференциално-термичен анализ. Установено е, че термичната стабилност на стъкло, съдържащо Eu_2O_3 драстично нараства. Оптичните спектри, показват, че стъклата са прозрачни във видимата област на спектъра. Установено е, че стъклокристалните образци, съдържащи $\text{LaVO}_3\text{:Eu}^{3+}$ се характеризират с повишена червена емисия ${}^5\text{D}_0\text{-}{}^7\text{F}_2$ в сравнение със стъклото. Това може да се обясни с по-ниската локална симетрия на Eu^{3+} йоните в кристалната фаза в сравнение със стъклото.